

Learning Collision-free and Torque-limited Robot Trajectories based on Alternative Safe Behaviors

Jonas C. Kiemel¹ and Torsten Kröger

Abstract—This paper presents an approach to learn online generation of collision-free and torque-limited robot trajectories. In order to generate future motions, a neural network is periodically invoked. Based on the current kinematic state of the robot and the network prediction, a trajectory for the current time interval can be calculated. The main idea of our paper is to execute the predicted motion only if a collision-free and torque-limited way to continue the trajectory is known. In practice, the motion predicted for the current time interval is extended by a braking trajectory and simulated using a physics engine. If the simulated trajectory complies with all safety constraints, the predicted motion is carried out. Otherwise, the braking trajectory calculated in the previous time interval serves as an alternative safe behavior. Given a task-specific reward function, the neural network is trained using reinforcement learning. The design of the action space used for reinforcement learning ensures that all predicted trajectories comply with kinematic joint limits. For our evaluation, simulated industrial robots and humanoid robots are trained to reach as many randomly placed target points as possible. We show that our method reliably prevents collisions with static obstacles and collisions between the robot arms, while generating motions that respect both torque limits and kinematic joint limits. Experiments with a real robot demonstrate that safe trajectories can be generated in real-time.

I. INTRODUCTION

In the manufacturing industry, industrial robots are frequently used for tasks like welding and spray painting. Typically, a repetitive motion sequence is hard-coded for each robot prior to putting a new production line into operation. This process is time-consuming and inflexible as the robots cannot react to unforeseen events or changes in their environment. Generating adaptive motions through reinforcement learning is a promising approach and an active field of research [1]–[3]. However, robots have to be able to explore their environment in order to learn well-performing motions. When starting learning from scratch, completely random actions are predicted at the beginning of the training process. Robots in production lines are usually placed close together and likely to collide if random motions are performed. In order to prevent damage to the robots and their environment, care must be taken to avoid collisions during the training process. Aside from collisions, a robot can also be damaged if one of its joints is overloaded. The kinematic capabilities of an industrial robot are limited by the maximum position θ , velocity $\dot{\theta}$, acceleration $\ddot{\theta}$ and jerk $\dddot{\theta}$ of each joint, whereas the dynamic potential is restricted by the maximum torque τ

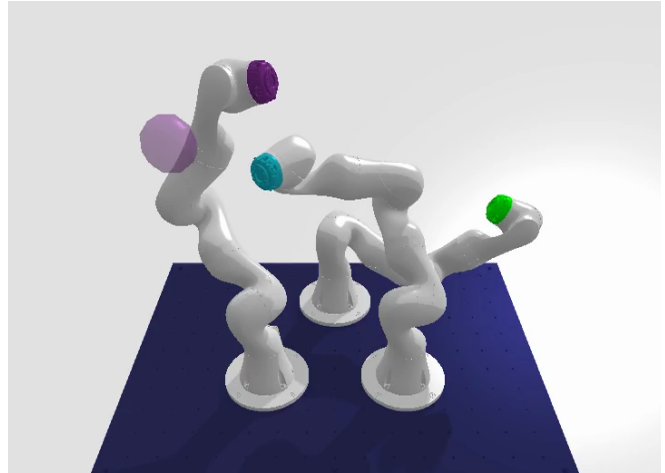


Fig. 1: By preventing collisions and torque limit violations, our method enables the learning of safe robot motions with multiple robot arms.

of each actuator. In this work, we consider a motion as safe, if no collision occurs and if no kinematic joint limit or torque limit is violated. For online trajectory generation, it is not sufficient to check whether all safety constraints are met within the current decision step as inevitable safety violations might occur at a later point in time. Consequently, a robotic system must check compliance with safety constraints over an infinite time-horizon or until a safe goal state is found [4]. A fundamental problem with online trajectory generation is that the safety of all subsequent movements must be guaranteed, although future movements cannot be predicted in advance. To overcome this problem, our work combines two ideas:

- Compliance with kinematic joint limits is ensured over an infinite time-horizon by the design of the action space used for reinforcement learning.
- Collisions and torque limit violations are prevented by ensuring the existence of an alternative safe behavior at each decision step.

With our approach, arbitrary movements can be predicted by a neural network without having to worry about potential safety implications. In the sections that follow, we clarify how alternative safe behaviors are generated and demonstrate the effectiveness of our method by learning various reaching tasks with up to three simulated robots. Experiments with a real robot are performed to show that safe motions can be computed in real-time. Our source code and our trained neural networks are publicly available.²

¹Institute for Anthropomatics and Robotics – Intelligent Process Automation and Robotics (IAR-IPR), Karlsruhe Institute of Technology (KIT), jonas.kiemel@kit.edu

²www.github.com/translearn/safeMotions

II. RELATED WORK

A. Safe reinforcement learning

The term safe reinforcement learning refers to methods that aim at respecting safety constraints during the learning phase and the deployment process [5]. Although reinforcement learning (RL) is widely used in robotics, safe learning is still considered as an outstanding challenge for practical applications [6]. One important aspect of safe reinforcement learning is the problem of safe exploration. In order to find well-performing policies, an RL agent has to explore its environment. During this process, dangerous situations have to be avoided. An overview of different techniques for safe exploration is given in [5] and [7]. To consider safety constraints during learning, the concept of Constrained Markov decision processes (CMDP) [8] was introduced and RL algorithms for CMDPs were developed [9]. In [10], several constrained and unconstrained RL algorithms are benchmarked in various environments. It is shown that the use of constrained RL algorithms does not guarantee strict constraint satisfaction, especially at the beginning of the training process. In contrast, our method ensures safety right from the beginning of the training process and even if the environment is modified afterwards.

B. Learning safe motions in robotics

Applying the concept of safe RL to robotics usually leads to the problem of safe online trajectory generation. When working with industrial robots, relevant safety constraints include the prevention of collisions and compliance with kinematic and dynamic joint limits. We note that jerk limits are often ignored by academic prototypes, although jerky movements may damage the gear boxes and actuators of a robot [6]. While most neural networks are trained in simulation environments [10], safety constraints become crucial as soon as motions are to be carried out by real robots. Practitioners have developed various techniques to avoid unsafe behaviors when performing real-world experiments. For instance, penalties for undesired behaviors can be added to the reward function of an unconstrained Markov decision process (MDP) [11], [12]. While penalties reduce the likelihood of undesirable behaviors, they do not provide strict safety guarantees, even if the training process is carried out until convergence [13]. Besides, undesirable behaviors at the beginning of the training process cannot be prevented by penalties. In some cases, task-specific heuristics can be used to avoid unsafe behaviors [1]. Designing the action space in such a way that all actions can be safely executed is an elegant solution to deal with safety constraints. However, this approach is often very restrictive and not suitable for all types of constraints [6]. An action space representation to ensure compliance with kinematic joint constraints was proposed in [13]. Conflicting constraints are avoided over an infinite time-horizon without restricting the workspace of the robot. We utilize the code provided by [13] for our action space representation and to generate braking trajectories. When considering kinematic joint constraints only, all joints can

be treated as decoupled. However, preventing collisions and torque limit violations is more challenging as the coupling between the joints has to be taken into account. While most online collision avoidance methods are based on potential fields [14]–[16], Faverjon and Tournassoud’s method [17] provides a way to avoid collisions by specifying explicit inequality constraints. In [18], Faverjon and Tournassoud’s method was applied to a reinforcement learning problem. The basic idea is to define and solve a quadratic program (QP) at each decision step. The QP outputs the closest action to the network prediction that satisfies the specified inequality constraints. As the constraint satisfaction is ensured for the current decision step only, this approach is computationally efficient. However, as stated in [4], a robotic system has to reason over an infinite time-horizon or until a safe goal state is found in order to avoid conflicting constraints. In the case of conflicting constraints, the QP has no solution and compliance with the safety constraints is no longer guaranteed. The more robot links are taken into account, the more constraints are required, and the more likely conflicting constraints become, especially if non strictly convex object shapes are considered [19]. Facing the problem of conflicting constraints when tracking Cartesian velocities, the concept of alternative safe behaviors was proposed in [20]. We adapt the concept of alternative safe behaviors to reinforcement learning and demonstrate its applicability to robotic systems with up to 33 degrees of freedom (DOF). Compared to [20], we additionally consider torque constraints, jerk limits and collisions between multiple robots.

III. APPROACH

A. Problem statement

Our method addresses the problem of learning collision-free robot motions complying with kinematic and dynamic joint limits. The following kinematic constraints are defined for each revolute or prismatic robot joint:

$$p_{min} \leq \theta \leq p_{max} \quad (1)$$

$$v_{min} \leq \dot{\theta} \leq v_{max} \quad (2)$$

$$a_{min} \leq \ddot{\theta} \leq a_{max} \quad (3)$$

$$j_{min} \leq \dddot{\theta} \leq j_{max}, \quad (4)$$

with θ being the joint position and p , v , a and j standing for position, velocity, acceleration and jerk, respectively. In addition, we specify torque limits for each actuator:

$$\tau_{min} \leq \tau \leq \tau_{max} \quad (5)$$

While the kinematic joint limits are defined with respect to the setpoints that are given to a joint trajectory controller, the torque limits refer to actual values. In order to avoid collisions, we observe the minimum distance between obstacle-link pairs and link-link pairs. An obstacle-link pair can be defined to prevent collisions between a robot link and an obstacle. Link-link pairs are used to prevent either self-collisions or collisions between different robots. The minimum distance between the observed pairs is checked at discrete time points with an adjustable frequency f_C .

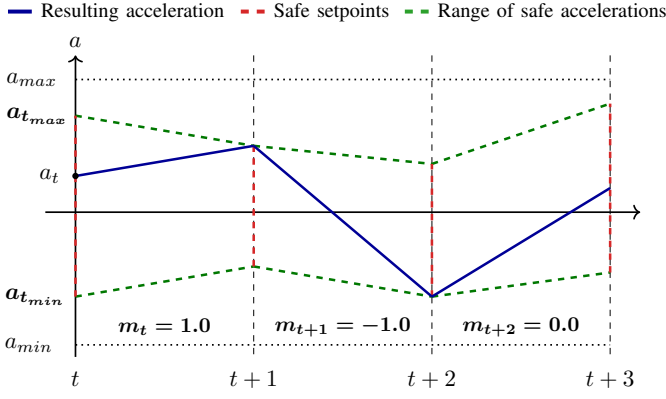


Fig. 2: For each joint and at each time step t , the desired joint acceleration a_{t+1_N} is determined by mapping a scalar m_t onto kinematically safe acceleration setpoints.

A trajectory is considered as unsafe, if the computed minimum distance is smaller than a user-specified safety distance d_S . In the presence of arbitrarily moving obstacles, collision avoidance cannot be guaranteed [4]. Therefore, we assume that our environment is composed of controllable robots and static obstacles only. In addition, the shape and the position of each object are known.

To learn motions with model-free RL, we define an unconstrained Markov decision process $(S, \mathcal{A}, P_{\underline{a}}, R_{\underline{a}})$, where S is the state space, \mathcal{A} is the action space, $P_{\underline{a}}$ are unknown transition probabilities and $R_{\underline{a}}$ is the immediate reward resulting from action \underline{a} . A neural network is trained to predict actions that maximize the sum of immediate rewards. The state $s \in S$ contains the current kinematic state of each robot joint (position p_t , velocity v_t , acceleration a_t) as well as additional task-specific information. The neural network predicts a single scalar $m_t \in [-1, 1]$ per joint as action $\underline{a} \in \mathcal{A}$. The immediate reward results from a task-specific reward function, which specifies the optimization goal of the learning problem. For our experiments, the prediction frequency f_N of the neural network is set to 10 Hz.

B. Adherence to kinematic constraints

In order to ensure compliance with kinematic joint constraints, we use the method described in [13] to compute for each joint the minimum and maximum acceleration $a_{t+1_{min}}$ and $a_{t+1_{max}}$ allowed at the beginning of the following time interval $t+1$. Since all intermediate acceleration setpoints lead to kinematically feasible trajectories, the desired acceleration at the beginning of the next time interval a_{t+1_N} can be computed by linearly mapping the network prediction $m_t \in [-1, 1]$ onto the range specified by $a_{t+1_{min}}$ and $a_{t+1_{max}}$:

$$a_{t+1_N} = a_{t+1_{min}} + \frac{1 + m_t}{2} \cdot (a_{t+1_{max}} - a_{t+1_{min}}) \quad (6)$$

$a_{t+1_{min}}$ and $a_{t+1_{max}}$ depend on the current kinematic state (p_t, v_t, a_t) and the specified kinematic limits (1) - (4). In Fig. 2, the resulting safe acceleration setpoints are visualized by red lines. To generate a continuous trajectory between the discrete decision steps, a linear interpolation between a_t and

Algorithm 1: Computing a safe value for a_{t+1}

at each time step t do

```

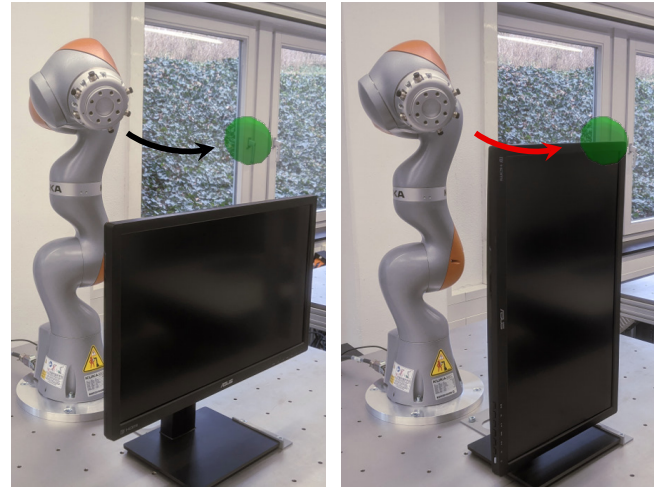
    compute  $a_{t+1_N}$  based on the network output  $m_t$ ;
    compute braking accelerations starting from
       $a_{t+1_N}$ : ( $a_{t+2_B}, a_{t+3_B}, \dots$ );
    alternative behavior  $\leftarrow$ 
      trajectory( $a_t, a_{t+1_N}, a_{t+2_B}, a_{t+3_B}, \dots$ );
    if alternative behavior is safe then
      |  $a_{t+1} \leftarrow a_{t+1_N}$ ;
    else
      | compute braking acceleration  $a_{t+1_B}$ ;
      |  $a_{t+1} \leftarrow a_{t+1_B}$ ;

```

a_{t+1} is performed. The corresponding joint velocities and joint positions can then be calculated by integration.

C. Prevention of collisions and torque limit violations

Collisions and torque limit violations are prevented by ensuring the existence of an alternative safe behavior prior to executing the motion resulting from the network prediction (Algorithm 1). The network prediction specifies the desired motion from the beginning of the current time interval t to the beginning of the next time interval $t+1$. To ensure the existence of a safely executable trajectory at $t+1$, the predicted motion is continued by a braking trajectory that stops all robot joints. Starting from the current kinematic state at t , the resulting movement is simulated and checked for collisions and torque limit violations. If no violations occur, an alternative safe behavior is found and the predicted motion is carried out until $t+1$. Otherwise, a braking trajectory is executed. In the following, the concept of alternative safe behaviors is further elaborated using a real-world example. An industrial robot is trained to reach randomly sampled target points in an environment in which a monitor is placed



(a) The target point is reached.

(b) The robot stops.

Fig. 3: Collisions are prevented even if the shape of an obstacle is changed from (a) to (b) after training.

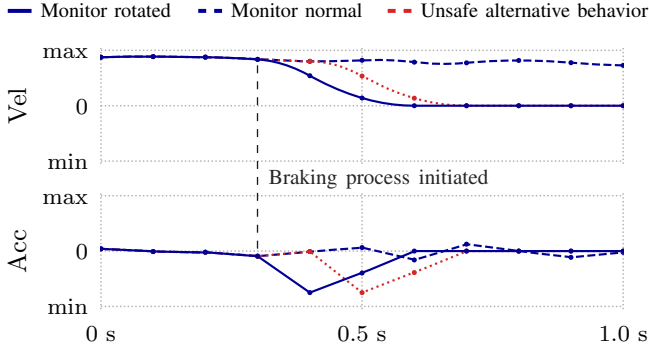


Fig. 4: After rotating the monitor (Fig. 3b), the alternative behavior computed at $t=0.3$ s leads to a collision. Thus, a braking process is initiated. Only one joint shown for clarity.

as an obstacle. As shown in Fig. 3, the orientation of the monitor is changed after training so that the desired target point can no longer be reached. The resulting trajectories for both monitor orientations are visualized in Fig. 4 and in the accompanying video³. In case of the rotated monitor shown in Fig. 3b, a braking process is initiated at $t=0.3$ s since the computed alternative behavior leads to a collision. Note that the finally executed braking trajectory is guaranteed to be collision-free as it was checked for safety violations in the previous decision step at $t=0.2$ s.

It is important to note that the robot does not necessarily come to a standstill when a braking process is initiated. If an alternative safe behavior is found in a subsequent decision step, the braking process is stopped and the motion is continued as predicted by the neural network. Fig. 5 shows an exemplary trajectory generated by selecting random actions. Although torque limit violations are prevented, the robot joint does not come to a full stop.

D. Computation of alternative behaviors

Conflicting constraints are avoided by ensuring the existence of an alternative safe trajectory at each decision step. The alternative trajectory has to lead to a safe goal state without causing safety violations. Starting from the current decision step t , the neural network predicts a desired motion until $t+1$. In the absence of moving obstacles, a safe goal state is reached when all robot joints have been brought to a stop. The shorter the duration of the alternative trajectory, the less computational effort is required to verify its compliance with the safety constraints. Thus, we extend the predicted motion with a braking trajectory that is time-optimal with respect to the following predefined kinematic limits:

$$a_{min, brake} \leq \ddot{\theta} \leq a_{max, brake} \quad (7)$$

$$j_{min, brake} \leq \dddot{\theta} \leq j_{max, brake} \quad (8)$$

The kinematic limits for braking trajectories must be either equal to or smaller than the limits specified in (3) and (4). Formally, the calculated braking trajectory is the fastest trajectory to bring each joint to zero velocity and zero

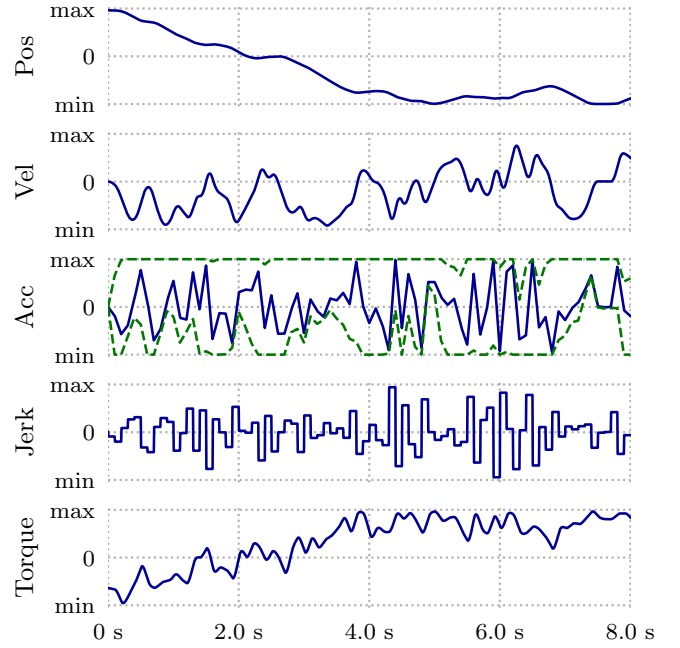


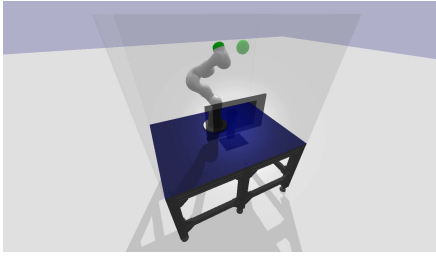
Fig. 5: Trajectory for a single joint generated by a random agent. The green lines visualize the range of kinematically safe accelerations. Note that the joint limits are not violated.

acceleration at the end of a time interval. The principle for calculating the required braking accelerations considering discrete decision steps is explained in [21]. If a desired braking acceleration is outside the range of safe accelerations shown in Fig. 2, the braking acceleration is clipped so that violations of the global kinematic limits (1) - (4) are prevented.

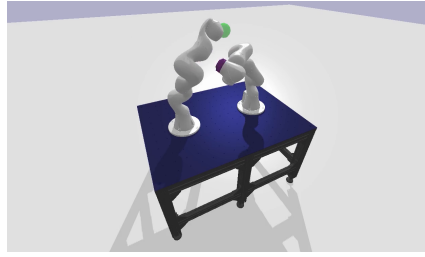
E. Checking alternative behaviors for collisions

Beginning with the current kinematic state at t , the alternative trajectory has to be checked for violations of the specified safety distance d_S . To do so, position setpoints are generated by sampling the alternative trajectory at a frequency of f_C . We assume that a kinematic model of the robot is given and that the shape and position of each obstacle are known. For every position setpoint, the distance between each observed obstacle-link pair and between each observed link-link pair is computed. We use the `getClosestPoints()` function provided by the physics engine PyBullet [22] to calculate the corresponding distances. If a single distance is smaller than the specified safety distance d_S , the whole trajectory is considered as unsafe and a braking process is initiated. Note that the computational effort depends on the duration of the alternative trajectory and the selected frequency of distance calculations f_C . For computational efficiency it is preferable to decrease the frequency f_C and to compensate the resulting inaccuracy by increasing the safety distance d_S . In our experiments, f_C is set to 100 Hz. Our collision avoidance method checks the setpoints of the alternative trajectory rather than the resulting actual values. Typically, trajectory tracking controller are able to closely follow the desired reference trajectory, so that the tracking

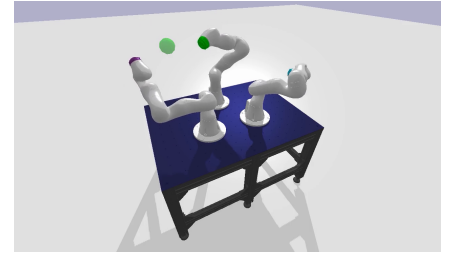
³<https://youtu.be/iZHmDjYfMF4>



(a) One industrial robot



(b) Two industrial robots



(c) Three industrial robots

Fig. 6: Industrial robots used for evaluation.

error can be compensated by defining a relatively small safety distance. If higher accuracy is required, the behavior of the trajectory controller can be approximated by a controller model. The resulting actual position values can then be pre-estimated and checked for violations of the safety distance.

F. Checking alternative behaviors for torque limit violations

The torque τ required to follow a desired joint acceleration $\ddot{\theta}$ can be computed using the dynamical model of rigid multi-bodies:

$$\tau = M(\theta)\ddot{\theta} + C(\theta, \dot{\theta})\dot{\theta} + G(\theta) + \tau_{ext}, \quad (9)$$

where M is the mass matrix, $C(\theta, \dot{\theta})\dot{\theta}$ represents centrifugal and Coriolis forces, $G(\theta)$ are gravity forces and τ_{ext} summarizes external contact forces. In order to detect potential torque limit violations, the execution of the alternative trajectory is simulated using the physics engine PyBullet. For our experiments, the simulation frequency f_S is set to 240 Hz. After every simulation step, the torque applied to each joint is read out and checked for compliance with the specified limits. While running a complete physics simulation is computational expensive, the approach is very flexible with regard to the observed constraint. For instance, the same principle could also be used to limit contact forces between the robot and elastic obstacles. Since collisions with static obstacles typically lead to torque limit violations, collisions can also be avoided by preventing torque limit violations. However, in contrast to the method described in III-E, no safety distance can be specified. Further distinguishing features between the two methods are listed in Table I. When applying our approach to real robots, the physics engine must be able to accurately model the forces resulting from the execution of the alternative behavior. In practice,

TABLE I: Collision prevention vs. Torque limit prevention

	Collision prevention	Torque limit prevention
Observed trajectory	setpoints	actual values
Test frequency	$f_C < f_S$	$f_S = 240$ Hz
	minimum distance	torque limit violations
	• to obstacles	for instance due to
	• between links	• high accelerations
Criteria for unsafe alternative behaviors	smaller than a safety distance d_S	• gravity
		• collisions

the simulation error can be compensated by subtracting a safety margin from the actual torque limits. If required, the simulation accuracy can also be improved based on system identification [2].

IV. EVALUATION

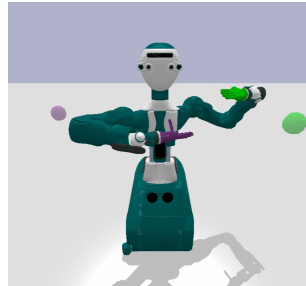
A. Environments used for evaluation

We evaluate our approach with various industrial robots and humanoid robots. The environments are shown in Fig. 6 and Fig. 7. Renderings are also provided in the accompanying video. TABLE II summarizes the most important properties of each environment.

TABLE II: Characteristics of our evaluation environments.

Environment	DOF	Obstacles	Obstacle-link pairs	Link-link pairs
Industrial				
• One robot	7	6	36	0
• Two robots	14	1	12	72
• Three robots	21	1	18	216
Humanoids				
• ARMAR-6	17	1	2	151
• ARMAR-6x4	33	1	4	610

The environment with a single ‘KUKA iiwa 7’ robot shown in Fig. 6a corresponds to our real-word setup depicted in Fig. 3. In this environment, the workspace of the robot is restricted by four virtual walls, a table and a monitor placed in front of the robot. Environments with two and three industrial robots are provided to demonstrate that our method can be applied to multiple robots sharing the same workspace.



(a) ARMAR-6



(b) ARMAR-6x4

Fig. 7: Humanoid robots used for evaluation.

TABLE III: Evaluation of our collision prevention method for random and for trained agents based on 900 episodes.

Configuration	Random agent			Trained agent						
	Target points	Closest	Adaptation	Target points					Closest	Adaptation
	Total	distance	rate	Total	Arm 1	Arm 2	Arm 3	Arm 4	distance	rate
One industrial robot										
• single target point	0.06	0.93 cm	12.9 %	8.90	8.90	–	–	–	0.88 cm	1.6 %
Two industrial robots										
• simultaneous target points	0.09	0.91 cm	8.1 %	10.46	2.08	8.38	–	–	0.62 cm	3.1 %
• alternating target points	0.04	0.93 cm	8.1 %	8.43	4.21	4.22	–	–	0.65 cm	2.3 %
Three industrial robots										
• simultaneous target points	0.10	0.82 cm	18.4 %	5.67	4.46	0.20	1.01	–	0.72 cm	17.2 %
• alternating target points	0.04	0.91 cm	18.6 %	5.07	1.68	1.75	1.64	–	0.71 cm	5.1 %
ARMAR-6										
• single target point	0.06	0.60 cm	5.6 %	13.06	6.33	6.73	–	–	0.95 cm	1.7 %
• simultaneous target points	0.05	0.79 cm	5.4 %	17.60	7.86	9.74	–	–	0.21 cm	7.0 %
• alternating target points	0.02	0.46 cm	5.5 %	12.40	6.22	6.18	–	–	0.62 cm	1.7 %
ARMAR-6x4										
• single target point	0.06	0.51 cm	22.8 %	7.95	0.07	0.01	4.09	3.78	0.32 cm	7.3 %
• simultaneous target points	0.10	0.45 cm	22.2 %	7.37	2.24	2.08	1.26	1.79	0.19 cm	27.2 %
• alternating target points	0.03	0.73 cm	22.8 %	5.53	1.37	1.41	1.36	1.39	0.38 cm	7.4 %

The maximum values for the position, velocity and torque of each joint are selected as specified by KUKA [23]. Acceleration limits are taken from a comparable Franka Emika robot [24] since no official data is provided by KUKA. The maximum jerk is limited through the linear interpolation of accelerations between decision steps and can be computed as follows:

$$\dot{j}_{max} = (a_{max} - a_{min}) \cdot f_N, \quad (10)$$

We also use our method to control both arms of the humanoid robot ARMAR-6 [25] without causing self-collisions. In order to demonstrate the scalability of our approach, we additionally introduce ‘ARMAR-6x4’, a four-armed modification of ARMAR-6 with 33 degrees of freedom.

B. Details of the learning process

Each of the robot arms is trained to reach randomly placed target points. The color of a target point indicates the robot arm to which the target point is assigned. As soon as a target point is reached, a new one is placed. We use three different variants to assign target points to the robot arms: In case of simultaneous target points, each robot arm has a dedicated target point. With alternating target points, one target point is assigned to the robots in alternating order. In case of the variant ‘single target point’, a single target point is assigned to all robot arms. The duration of each episode is set to eight seconds. All robot arms are controlled by a single agent. The performance of an agent is assessed based on the average number of target points reached within an episode. In our learning experiments, the agent is a neural network with 256 neurons in the first hidden layer and 128 neurons in the second hidden layer. The neural network is trained using an RL algorithm called Proximal Policy Optimization (PPO) [26]. The task-specific part of the state $s \in \mathcal{S}$ contains the Cartesian position of each target point and the relative

position between a target point and its corresponding robot arm. In case of alternating target points, an additional input signal indicates whether the target point is active or not. The reward function encourages a reduction of the distance between a target point and the corresponding robot arm and penalizes small distances between the observed obstacle-link pairs and link-link pairs.

C. Evaluation of our collision prevention method

The average performance of our collision prevention method is evaluated for various experimental configurations considering both random agents and trained agents. The results are shown in TABLE III. It can be seen that the average number of target points reached within one episode increases significantly during training. For both random agents and trained agents, the closest distance between the observed obstacle-link pairs and link-link pairs is always greater than zero, showing that collisions are entirely prevented. For all of our experiments, we specify a safety distance d_s of 1.0 cm. The closest distance is slightly smaller than the safety distance for two reasons: Firstly, the closest distance is measured at a frequency of $f_S = 240$ Hz, whereas the alternative behavior is checked for collisions at a rate of $f_C = 100$ Hz. Secondly, the closest distance refers to actual values whereas the safety distance is defined with respect to trajectory setpoints. The resulting inaccuracy can always be compensated by increasing the safety distance. The adaptation rate reflects the proportion of network predictions that is adapted by our method. The highest adaptation rate occurs in case of the four-armed robot ARMAR-6x4, indicating that this environment is particularly challenging. Interestingly, the four-armed robot uses only two of its arms if a single target point should be reached. The other two arms are stretched so that no collisions occur. We conclude that the additional arms are more of a burden than a help for this particular task.

TABLE IV: Ablation studies for collision prevention.

Configuration	Target points	Episodes with collisions	Adaptation rate
ARMAR-6 with simultaneous target points			
• Random agent without collision prevention	0.07	75.0 %	–
• Trained and evaluated without collision prevention	18.57	64.8 %	–
• Trained without collision prevention, evaluated with collision prevention	14.86	0.0 %	23.0 %
• Trained and evaluated with collision prevention	16.08	0.0 %	9.1 %
• Trained and evaluated with collision prevention using setpoints	17.60	0.0 %	7.0 %

To further analyze the impact of our method, we perform the ablation studies shown in TABLE IV. As expected, random agents and trained agents frequently cause collisions without collision prevention. It is possible to apply our method to an agent trained without collision prevention to enable safe deployment. In this case, collisions are prevented but the adaptation rate is rather high and the performance of the agent decreases. If our method is used during training and evaluation, the performance of the agent increases, as the neural network learns to avoid the execution of alternative behaviors. Since our method prevents collisions, the trajectory controller is able to accurately track the desired trajectory. For that reason, it is possible to use the trajectory setpoints rather than the actual values for the reward calculation. By doing so, the performance increases, as the delay caused by the trajectory controller is avoided. In summary, our method leads to a slight decrease in performance. However, the performance gap can be reduced by applying our method during training and evaluation and by utilizing that the reward for a collision-free trajectory can be assessed based on the trajectory setpoints rather than the actual values.

D. Evaluation of our torque limit prevention method

To evaluate the effectiveness of our method for preventing torque limit violations, we perform experiments with a single industrial robot and with the humanoid robot ARMAR-6. Performance metrics obtained by evaluating 900 episodes per experiment are shown in TABLE V. In a first experiment, the industrial robot is trained with collision prevention but without torque limit prevention. Compared to our previous experiments, the maximum torque of the robot joints τ_{max} is reduced by 40 %. Using this configuration, torque limit violations occur in more than half of the episodes. However, when evaluating the agent with both collision prevention and torque limit prevention, the torque limit violations no longer occur, while the impact on the performance is rather small. As explained in section III-F, collisions typically lead to torque limit violations. For that reason, collisions can also be avoided by preventing torque limit violations. Our experiments with the humanoid robot ARMAR-6 show that

TABLE V: Evaluation of the torque limit prevention.

Configuration	Target points	Episodes with collisions	torque violations
One industrial robot, maximum torque reduced by 40 %			
• Trained and evaluated with collision prevention only	8.90	0.0 %	52.3 %
• Trained with collision prevention, evaluated with collision prevention and torque limit prevention	8.20	0.0 %	0.0 %
ARMAR-6 with simultaneous target points			
• Random agent with torque limit prevention only	0.07	0.0 %	0.0 %
• Trained and evaluated with torque limit prevention	16.17	0.0 %	0.0 %

neither a random agent nor a trained agent causes collisions or torque limit violations when evaluated with our torque limit prevention method. However, compared to our collision prevention method, no safety distance is maintained. For experiments with real robots, the torque limit prevention should either be combined with our collision prevention method or the collision models of the robot links should be chosen slightly larger than their real counterparts.

E. Real-time capability and sim-2-real transfer

In order to apply our approach to real robots, alternative safe behaviors must be computed in real time. As a first step, we analyze the maximum computation time of simulated episodes with a duration of 8 s using an Intel i9-9900K CPU. The results are shown in TABLE VI. In all of our experiments, the computation takes less than 8 s per episode. Nevertheless, the collision prevention for ARMAR6-x4 is not real-time capable when checking collision with $f_C = 100$ Hz since real-time capability additionally implies that all calculations are available at the requested time. We note that the computational effort for collision prevention can be significantly reduced by decreasing f_C . In this case, the safety distance has to be increased to make sure that no collisions occur between the discrete collision checks. For real-time execution, two threads are started by our program: The first one computes the desired kinematic state at the end of the subsequent decision step $t+1$ and checks the resulting alternative behavior for safety violations.

TABLE VI: Maximum computation times for episodes with a duration of 8 seconds. Green values indicate real-time capability. Results based on 100 episodes.

Agent trained with a single target point	Industrial One robot	Humanoids	
		ARMAR-6	ARMAR-6x4
• Neither collision prevention nor torque limit prevention	0.57 s	0.65 s	0.70 s
• Collision prevention	0.96 s	2.43 s	7.82 s
• Torque limit prevention	1.31 s	2.63 s	6.10 s

As shown in Fig. 8, these computations are performed in advance to the actual decision step. In order to check the alternative safe behavior for torque violations, the actual position at decision step $t+1$ has to be known. To enable the desired precalculation, we model the behavior of the trajectory controller as a first order low-pass with a time constant of 30 ms. The second thread keeps synchronized with the trajectory controller of the real robot while interpolating position setpoints at a frequency of 200 Hz. As can be seen in the accompanying video, we successfully transferred a trained policy including collision prevention and torque limit prevention to a real industrial robot.

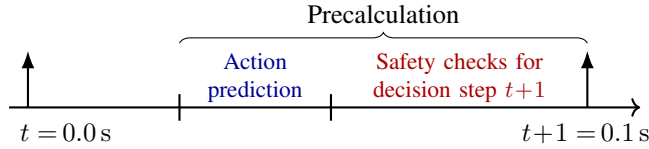


Fig. 8: Safety checks are performed in advance.

V. CONCLUSION AND FUTURE WORK

This paper presented a method to learn collision-free and torque-limited robot trajectories. Conflicting constraints are avoided by ensuring the existence of an alternative safe behavior at each decision step. Violations of kinematic joint limits are prevented by the design of the action space used for reinforcement learning. Our evaluation with up to three simulated robots showed that neither random agents nor trained agents violated the specified constraints. Experiments with a real industrial robot demonstrated that safe motions can be computed in real-time.

In future work, we would like to apply our approach to other constraints like Cartesian velocity limits and contact forces. In addition, we are interested in investigating more sophisticated alternative behaviors, for instance to apply our method to legged robots that cannot be stopped in unstable positions or to avoid moving obstacles.

ACKNOWLEDGMENT

This research was supported by the German Federal Ministry of Education and Research (BMBF) and the Indo-German Science & Technology Centre (IGSTC) as part of the project TransLearn (01DQ19007A). We appreciate the access to the KUKA Robot Learning Lab at KIT and thank Tamim Asfour for his valuable feedback and advice.

REFERENCES

- [1] S. Gu, E. Holly, T. Lillicrap, and S. Levine, "Deep reinforcement learning for robotic manipulation with asynchronous off-policy updates," in *2017 IEEE international conference on robotics and automation (ICRA)*. IEEE, 2017, pp. 3389–3396.
- [2] M. Kaspar, J. D. Muñoz Osorio, and J. Bock, "Sim2real transfer for reinforcement learning without dynamics randomization," in *2020 IEEE/RSJ International Conference on Intelligent Robots and Systems (IROS)*, 2020, pp. 4383–4388.
- [3] G. Thomas, M. Chien, A. Tamar, J. A. Ojea, and P. Abbeel, "Learning robotic assembly from cad," in *2018 IEEE International Conference on Robotics and Automation (ICRA)*. IEEE, 2018, pp. 1–9.
- [4] T. Fraichard, "A short paper about motion safety," in *Proceedings 2007 IEEE International Conference on Robotics and Automation*, 2007, pp. 1140–1145.
- [5] J. Garcia and F. Fernández, "A comprehensive survey on safe reinforcement learning," *Journal of Machine Learning Research*, vol. 16, no. 1, pp. 1437–1480, 2015.
- [6] J. Ibarz, J. Tan, C. Finn, M. Kalakrishnan, P. Pastor, and S. Levine, "How to train your robot with deep reinforcement learning: lessons we have learned," *The International Journal of Robotics Research*, p. 027836492098785, Jan 2021. [Online]. Available: <http://dx.doi.org/10.1177/0278364920987859>
- [7] M. Pecka and T. Svoboda, "Safe exploration techniques for reinforcement learning—an overview," in *International Workshop on Modelling and Simulation for Autonomous Systems*. Springer, 2014, pp. 357–375.
- [8] E. Altman, *Constrained Markov decision processes*. CRC Press, 1999, vol. 7.
- [9] J. Achiam, D. Held, A. Tamar, and P. Abbeel, "Constrained policy optimization," in *International Conference on Machine Learning*, 2017, pp. 22–31.
- [10] A. Ray, J. Achiam, and D. Amodei, "Benchmarking safe exploration in deep reinforcement learning," *arXiv preprint arXiv:1910.01708*, 2019.
- [11] J. Tan, T. Zhang, E. Coumans, A. Iscen, Y. Bai, D. Hafner, S. Bohez, and V. Vanhoucke, "Sim-to-real: Learning agile locomotion for quadruped robots," *arXiv preprint arXiv:1804.10332*, 2018.
- [12] O. M. Andrychowicz, B. Baker, M. Chociej, R. Jozefowicz, B. McGrew, J. Pachocki, A. Petron, M. Plappert, G. Powell, A. Ray, et al., "Learning dexterous in-hand manipulation," *The International Journal of Robotics Research*, vol. 39, no. 1, pp. 3–20, 2020.
- [13] J. C. Kiemel and T. Kröger, "Learning robot trajectories subject to kinematic joint constraints," in *2021 International Conference on Robotics and Automation (ICRA)*, 2021.
- [14] O. Khatib, "Real-time obstacle avoidance for manipulators and mobile robots," in *Autonomous robot vehicles*. Springer, 1986, pp. 396–404.
- [15] C. W. Warren, "Global path planning using artificial potential fields," in *1989 IEEE International Conference on Robotics and Automation*. IEEE Computer Society, 1989, pp. 316–317.
- [16] F. Flacco, T. Kröger, A. De Luca, and O. Khatib, "A depth space approach to human-robot collision avoidance," in *2012 IEEE International Conference on Robotics and Automation*. IEEE, 2012, pp. 338–345.
- [17] B. Faverjon and P. Tournassoud, "A local based approach for path planning of manipulators with a high number of degrees of freedom," in *Proceedings. 1987 IEEE international conference on robotics and automation*, vol. 4. IEEE, 1987, pp. 1152–1159.
- [18] T.-H. Pham, G. De Magistris, and R. Tachibana, "Optlayer-practical constrained optimization for deep reinforcement learning in the real world," in *2018 IEEE International Conference on Robotics and Automation (ICRA)*. IEEE, 2018, pp. 6236–6243.
- [19] F. Kanehiro, F. Lamiraux, O. Kanoun, E. Yoshida, and J.-P. Laumond, "A local collision avoidance method for non-strictly convex polyhedra," *Proceedings of robotics: science and systems IV*, p. 33, 2008.
- [20] S. Rubrecht, V. Padois, P. Bidaud, M. De Broissia, and M. D. S. Simoes, "Motion safety and constraints compatibility for multibody robots," *Autonomous Robots*, vol. 32, no. 3, pp. 333–349, 2012.
- [21] J. C. Kiemel, R. Weitemeyer, P. Meißner, and T. Kröger, "True/Adapt: Learning smooth online trajectory adaptation with bounded jerk, acceleration and velocity in joint space," in *2020 IEEE/RSJ International Conference on Intelligent Robots and Systems (IROS)*, 2020, pp. 5387–5394.
- [22] E. Coumans and Y. Bai, "Pybullet, a python module for physics simulation for games, robotics and machine learning," 2016.
- [23] "Kuka sensitive robotics lbr iiwa," p. 30, 2017. [Online]. Available: https://www.kuka.com/-/media/kuka-downloads/imported/9cb8e311bfd744b4b0eab25ca883f6d3/kuka_lbr_iiwa_brochure_en.pdf
- [24] "Franka emika robot and interface specifications," 2017. [Online]. Available: https://frankaemika.github.io/docs/control_parameters.html
- [25] T. Asfour, L. Kaul, M. Wächter, S. Ottenhaus, P. Weiner, S. Rader, R. Grimm, Y. Zhou, M. Grotz, F. Paus, et al., "Armar-6: A collaborative humanoid robot for industrial environments," in *2018 IEEE-RAS 18th International Conference on Humanoid Robots (Humanoids)*. IEEE, 2018, pp. 447–454.
- [26] J. Schulman, F. Wolski, P. Dhariwal, A. Radford, and O. Klimov, "Proximal policy optimization algorithms," *arXiv preprint arXiv:1707.06347*, 2017.